



Published in final edited form as:

*Angiogenesis*. 2012 September ; 15(3): 443–455. doi:10.1007/s10456-012-9272-2.

## Equal modulation of endothelial cell function by four distinct tissue-specific mesenchymal stem cells

**Ruei-Zeng Lin,**

Department of Cardiac Surgery, Children's Hospital Boston, Harvard Medical School, 300 Longwood Ave., Boston, MA 02115, USA

**Rafael Moreno-Luna,**

Department of Cardiac Surgery, Children's Hospital Boston, Harvard Medical School, 300 Longwood Ave., Boston, MA 02115, USA. Unidad Clínico-Experimental de Riesgo Vascular (UCAMI-UCERV), Servicio de Medicina Interna, Hospital Universitario Virgen del Rocío, and Instituto de Biomedicina de Sevilla (IBiS), 41013 Seville, Spain

**Bin Zhou,**

Department of Cardiology, Children's Hospital Boston, Harvard Medical School, 300 Longwood Ave., Boston, MA 02115, USA. Key Laboratory of Nutrition and Metabolism, Institute for Nutritional Sciences, Shanghai Institutes for Biological Sciences, Chinese Academy of Sciences, Shanghai 200031, China

**William T. Pu, and**

Department of Cardiology, Children's Hospital Boston, Harvard Medical School, 300 Longwood Ave., Boston, MA 02115, USA

**Juan M. Melero-Martin**

Department of Cardiac Surgery, Children's Hospital Boston, Harvard Medical School, 300 Longwood Ave., Enders 349, Boston, MA 02115, USA

Juan M. Melero-Martin: [juan.meleromartin@childrens.harvard.edu](mailto:juan.meleromartin@childrens.harvard.edu)

### Abstract

Mesenchymal stem cells (MSCs) can generate multiple end-stage mesenchymal cell types and constitute a promising population of cells for regenerative therapies. Additionally, there is increasing evidence supporting other trophic activities of MSCs, including the ability to enable formation of vasculature *in vivo*. Although MSCs were originally isolated from the bone marrow, the presence of these cells in the stromal vascular fraction of multiple adult tissues has been recently recognized. However, it is unknown whether the capacity to modulate vasculogenesis is ubiquitous to all MSCs regardless of their tissue of origin. Here, we demonstrated that tissue-resident MSCs isolated from four distinct tissues have equal capacity to modulate endothelial cell function, including formation of vascular networks *in vivo*. MSCs were isolated from four murine tissues, including bone marrow, white adipose tissue, skeletal muscle, and myocardium. In culture, all four MSC populations secreted a plethora of pro-angiogenic factors that unequivocally induced proliferation, migration, and tube formation of endothelial colony-forming cells (ECFCs). *In vivo*, co-implantation of MSCs with ECFCs into mice generated an extensive network of blood vessels with ECFCs specifically lining the lumens and MSCs occupying perivascular positions.

© Springer Science+Business Media B.V. 2012

Correspondence to: Juan M. Melero-Martin, [juan.meleromartin@childrens.harvard.edu](mailto:juan.meleromartin@childrens.harvard.edu).

Electronic supplementary material The online version of this article (doi:10.1007/s10456-012-9272-2) contains supplementary material, which is available to authorized users.

**Conflict of interest** The authors have declared that no conflict of interest exists.

Importantly, there were no differences among all four MSCs evaluated. Our studies suggest that the capacity to modulate the formation of vasculature is a ubiquitous property of all MSCs, irrespective of their original anatomical location. These results validate multiple tissues as potential sources of MSCs for future cell-based vascular therapies.

## Keywords

Mesenchymal stem cells; Endothelial cell; Vasculogenesis; Pericytes; Endothelial progenitor cells

---

## Introduction

Mesenchymal stem cells (MSCs) are a subset of multipotent precursors that reside in the stromal fraction of many postnatal tissues. MSCs can differentiate into distinctive end-stage mesenchymal cell types, including those found in fat, bone, and cartilage [1]. Due to their multilineage differentiation potential, as well as ease of isolation and expansion, MSCs are the subject of intensive clinical research and constitute a promising cell population for future regenerative therapies [2].

MSCs were first identified in the bone marrow stroma as a population of fibroblast-like cells that adhered with ease to tissue culture plates and were able to differentiate into multiple mesenchymal cell types [3–5]. However, the bone marrow is not the only tissue that contains cells with these characteristics; there are now numerous studies that demonstrate the presence of MSCs in a diverse range of human tissues, including adipose tissue, skeletal muscle, and placenta [6, 7]. The identity of MSCs in vivo, their anatomical localization, as well as their functional roles in tissue homeostasis have become increasingly better understood [8]. In this regard, Crisan et. al. demonstrated that multiple human tissues contain subpopulations of perivascular cells that express MSC markers in situ and retain multilineage differentiation potential following expansion in culture, thus revealing a close connection between MSCs and pericytes [6, 9]. From a practical standpoint, definition of a MSC is often simplified to a multilineage differentiation ability after in vitro expansion. However, this definition is not sufficient to indicate whether MSCs from different anatomical locations have an equivalent therapeutic potential. For example, MSCs isolated from both bone marrow and adipose tissue have multipotential capacity but exhibit differential sensitivities to inductive molecules in culture [10], which reflects the influence of their tissue of origin. Additionally, MSCs derived from various postnatal and embryonic tissues display significant differences in colony morphology, differentiation potential, and gene expression [7, 11–13]. Moreover, equivalent multipotential ability in vitro does not necessarily imply equivalent cell performance upon engraftment in vivo. Thus, there are multiple questions regarding differential properties of distinct tissue-resident MSCs that remain unanswered.

The therapeutic potential of MSCs is more extensive than solely the capacity to generate large number of multiple end-stage mesenchymal cell types (e.g., adipocytes, chondrocytes, and osteocytes) [14]. There is increasing evidence supporting additional trophic and immunomodulatory activities of MSCs, including the ability to enable de novo formation of microvascular networks in vivo. For example, studies have demonstrated that bone marrow-derived MSCs facilitate the self-assembly of human blood-derived endothelial colony-forming cells (ECFCs) and umbilical cord vein endothelial cells (HUVECs) into functional capillaries in models of human cell implantation in immunodeficient mice [15, 16]. Similar properties have also been described using MSCs from white adipose tissue [17]. However, the influence of the tissue of origin on the vascular modulatory properties of cultured MSCs remains largely unknown.

Here, we demonstrate that MSCs isolated from four distinct tissues have equal capacity to facilitate the generation of functional human vasculature *in vivo*. The tissues examined were murine bone marrow, white adipose tissue, skeletal muscle, and myocardium. Our studies suggest that the capacity to modulate the formation of vasculature is a ubiquitous property of all MSCs, irrespective of their anatomical location.

## Materials and methods

### Isolation of stromal vascular fraction from murine tissues

Mouse stromal vascular fractions (SVFs) of four different tissues were isolated from six-week-old C57BL/6 and GFP-C57BL/6 mice (Jackson Laboratories) as follows:

**Bone marrow**—Hind limbs were dissected from the trunk of euthanized mice and muscle and connective tissues were removed to obtain tibia and femur bones. Bones were digested (1 mg/mL collagenase A, 2.5 U/mL dispase, 126  $\mu$ M calcium chloride, and 80  $\mu$ M magnesium sulfate in DMEM containing 1 % FBS) for 10 min at 37 °C. Bones were then crushed with a glass pestle and digested for an additional 30 min. The SVF was obtained after removal of bone fragments with a 100- $\mu$ m cell strainer and lysis of erythrocytes with ammonium chloride solution.

**White adipose tissue**—Subcutaneous white fat pads were excised from euthanized mice, minced, and digested for 1 h at 37 °C. The SVF was obtained after removal of mature adipocytes by centrifugation (450 $\times$ *g* for 10 min) and the lysis of erythrocytes with ammonium chloride solution.

**Myocardium and skeletal muscle**—Myocardium and skeletal muscle tissues were excised from the hearts and hind limbs of euthanized mice, respectively. Pericardial and adipose tissues were carefully removed from the harvested tissues prior to digestion. Tissues were minced and digested for 1 h at 37 °C. The digested cells and tissues were then collected by centrifugation and digested for an additional 1 h. The SVFs were obtained following the removal of undigested tissues with a 100- $\mu$ m cell strainer and lysis of erythrocytes with ammonium chloride solution.

### Purification and culture of MSCs

The SVFs were plated on uncoated tissue culture dishes using MSC-medium: MSC-GM Mesenchymal Stem Cell Medium BulletKit (basal media and SingleQuots; Lonza), supplemented with 10 % FBS (MSC-Qualified; Gibco/Invitrogen), 1 $\times$  Penicillin–streptomycin–glutamine solution (PSG), and 10 ng/mL of FGF-2 (R&D system). After 48 h, unbound cells were removed. Thereafter, medium was replaced every 2 days. Once each SVF culture reached 80 % confluence, cells were detached and incubated with a FITC-conjugated anti-mouse CD45 antibody (1  $\mu$ L for  $1 \times 10^6$  cells), followed by anti-FITC magnetic microbeads (Miltenyi Biotec), and passed through magnetic columns (Miltenyi Biotec). The CD45<sup>-</sup> cell fraction were then incubated with a PE-conjugated anti-PDGFR- $\beta$  antibody (5  $\mu$ L for  $1 \times 10^6$  cells), followed by anti-PE magnetic microbeads, and passed through magnetic columns (Fig. 1a). The purified CD45<sup>-</sup>/PDGFR- $\beta$ <sup>+</sup> MSCs (referred to here as tissue-resident MSCs) were cultured on uncoated tissue culture dishes using MSC-medium. All experiments were carried out with MSCs at passage 3.

### Flow cytometry and indirect immunofluorescence

MSCs at passage 3 were characterized by standard flow cytometry (CD45, CD11b, CD34, CD31, PDGFR- $\beta$ , CD146, CD90, Sca-1, CD29, and CD44) and indirect immunofluorescent staining (vimentin and  $\alpha$ -SMA) as previously described [18, 19]. Mouse dermal endothelial

cells (mDEC) and peripheral blood leukocytes served as controls. Antibodies and staining dilutions were summarized in Supplemental Table 1.

### Multilineage differentiation of MSCs

**Adipogenesis**—Confluent MSCs were cultured for 10 days in low-glucose DMEM with 10 % FBS, 1× GPS, and adipogenic supplements (5 µg/mL insulin, 1 µM dexamethasone, 0.5 mM isobutylmethylxanthine, 60 µM indomethacin, 1 µM rosiglitazone). Differentiation into adipocytes was assessed by Oil Red O staining. Cells cultured in medium lacking adipogenic supplements served as a negative control.

**Osteogenesis**—Confluent MSCs were cultured for 21 days in low-glucose DMEM with 10 % FBS, 1× GPS, and osteogenic supplements (1 µM dexamethasone, 10 mM β-glycerophosphate, 60 µM ascorbic acid-2-phosphate). Differentiation into osteocytes was assessed by alkaline phosphatase and von Kossa staining. Cells cultured in medium lacking osteogenic supplements served as a negative control.

**Chondrogenesis**—Suspensions of MSCs were gently centrifuged in 15 mL polypropylene centrifuge tubes (500,000 cells/tube). The pellets were cultured in high-glucose DMEM medium with 1× GPS, and chondrogenic supplements (1× insulin–transferrin–selenium, 1 µM dexamethasone, 100 µM ascorbic acid-2-phosphate, and 10 ng/mL TGF-β3). After 21 days, pellets were fixed in 10 % buffered formalin, cryoprotected in 30 % (w/v) sucrose solution, embedded in O.C.T. medium, and sectioned (8 µm-thick) using a cryostat microtome. Differentiation into chondrocytes was assessed by evaluating the presence of glycosaminoglycans after Alcian Blue staining. Cells cultured in the absence of TGF-β3 served as negative controls and failed to form compact spheroids.

**Smooth muscle myogenesis**—MSCs were co-cultured for 7 days with mDEC (1:1 ratio) on fibonectin-coated, 2-well Permaxox chamber slides at a density of  $1 \times 10^5$  cell/well using EGM-2 medium (Lonza). MSC expression of smooth muscle myosin heavy chain (smMHC) was evaluated by immunofluorescence using a rabbit monoclonal antibody followed by anti-rabbit Texas Red-conjugated secondary antibody. mDECs were stained with FITC-conjugated isolectin Griffonia simplicifolia B4 (IB4; 1:200; Vector Laboratories). Monocultures of MSCs cultured in EGM-2 medium served as negative control.

### Angiogenesis assays

Confluent cultures of MSCs were incubated in EBM-2, 5 % FBS (basal medium) for 24 h. MSC conditioned medium (MSC-CM) was filtered (0.2 µm) and concentrated (Amicon Ultra centrifugal filters, Regenerated cellulose; 3 kDa cut off; Millipore) to a tenfold reduced volume. MSC-CM was reconstituted in basal medium (1:10) prior to use. Proliferation assays were carried out with ECFCs seeded in triplicate onto fibonectin-coated 24-well plates at  $5 \times 10^3$  cell/cm<sup>2</sup> using basal medium; plating efficiency was determined at 24 h; cells were then treated for 48 h using basal medium in the presence or absence of either 10 ng/mL VEGF-A (R&D Systems) and 1 ng/mL bFGF (R&D Systems), or conditioned media. Cells were stained with DAPI and counted under a fluorescent microscope. The scratch assay was performed in confluent cultures of ECFCs plated on a 6-well plate. Scratch wounds were generated across each well using a pipette tip. Scratch size was measured after 48 h for each culture condition. The sprouting assay was performed with ECFC-coated microcarriers embedded in fibrin gel (2 mg/mL of fibrinogen, 0.15 U/mL of aprotinin, and 0.625 U/mL of thrombin) for 4 days, as previously described [19]. To coat microcarriers, ECFCs were mixed with Cytodex 3 microcarriers (Amersham Pharmacia Biotech) at a concentration of 200 ECFCs per bead. Beads with cells were shaken gently

every 30 min for 3 h at 37 °C and 5 % CO<sub>2</sub> to allow uniform ECFC coating. The following day, beads with cells were washed three times with EGM-2 before gel embedding. The tube formation assay was carried out by seeding ECFCs on Matrigel-coated plates at a density of  $2 \times 10^4$  cell/cm<sup>2</sup>. After incubating for 24 h in each culture condition, the total length of ECFC-lined cords were measured using ImageJ analysis software (NIH, Bethesda, MD, USA), as previously described [19]. Secretion of angiogenic factors was evaluated in each MSC-CM sample with mouse angiogenesis antibody arrays (R&D Systems), as described in the manufacturer's manual. Antigen-antibody complexes were visualized using Lumiglo (KPL) and chemiluminescent sensitive film (Kodak). Densitometry was performed by image analysis to quantify the amount of protein present in each MSC-CM sample (ImageJ).

### In vivo vasculogenic assay

Postnatal vasculogenesis is a paradigm in which circulating endothelial progenitor cells are recruited to form new blood vessels. The capacity of MSCs to support postnatal vasculogenesis in vivo was evaluated using our xenograft model of ECFC transplantation [18]. Briefly, MSCs isolated from GFP-C57BL/6 mice (GFP-MSCs) were combined with human cord blood-derived ECFCs ( $2 \times 10^6$  total; 40:60 ECFC/GFP-MSC ratio) in 200  $\mu$ L of Matrigel and the mixture subcutaneously injected into a 6-week-old male athymic nu/nu mouse (n = 4 for each GFP-MSC group). Implants were harvested after 7 days, fixed overnight in 10 % buffered formalin, embedded in paraffin and sectioned (7  $\mu$ m-thick). Hematoxylin and eosin (H&E) stained sections were examined for the presence of blood vessels containing red blood cells. Microvessel density (vessels/mm<sup>2</sup>) was reported as the average number of erythrocyte-filled vessels in sections from the middle of the implants. Immunofluorescent staining was performed on 7- $\mu$ m-thick sections were stained as previously described [15]. GFP-MSCs were stained with a rabbit anti-GFP antibody (1:2,000; abcam) followed by FITC-conjugated secondary antibody (1:200; Vector Laboratories). ECFC-lined microvessels were stained with a mouse anti-human CD31 antibody (1:50; abcam) followed by biotinylated IgG and Texas Red-conjugated streptavidin (1:200; Vector Laboratories). Alpha-smooth muscle actin ( $\alpha$ -SMA) was stained with an anti- $\alpha$ -SMA antibody (1:100; Sigma-Aldrich) followed by a Texas Red-conjugated secondary antibody (1:200; Vector Laboratories). All sections were counterstained with DAPI (Vector Laboratories).

### Statistical analysis

Data were expressed as mean  $\pm$  SEM. Comparisons between groups were performed by ANOVA followed by Bonferroni post-test analysis using Prism Version 4 software (GraphPad).  $P < 0.05$  was considered statistically significant.

## Results

### Isolation and characterization of tissue-resident MSCs

Tissue-resident MSCs were isolated from the SVF of four different murine tissues: (1) bone marrow (bm), (2) white adipose tissue (wat), (3) skeletal muscle (skm), and (4) myocardium (myo). In all cases, the SVF was cultured until it reached 80 % confluence prior to selection of MSCs. Thereafter, MSCs were selected based on their negative expression of CD45 and positive expression of PDGFR- $\beta$  (Fig. 1a). This methodology resulted in highly homogenous CD45<sup>-</sup>/PDGFR- $\beta$ <sup>+</sup> MSC populations (>96 % purity in all cases; Fig. 1a) and eliminated the majority of cellular contaminants originally present in the SVF, including hematopoietic cells (CD45<sup>+</sup>), endothelial cells (ECs) (CD45<sup>-</sup>/PDGFR- $\beta$ <sup>-</sup>), and non-perivascular stromal cells (CD45<sup>-</sup>/PDGFR- $\beta$ <sup>-</sup>). Purified MSCs displayed a characteristic spindle-shape morphology in culture (Fig. 1b). The mesenchymal phenotype was confirmed by additional methods. Indirect immunofluorescent staining confirmed the uniform

expression of mesenchymal intermediate filament vimentin in all MSCs populations (Fig. 1c).  $\alpha$ -SMA, an intracellular marker often associated with cultured mesenchymal cells, was also visible in all MSCs, although its expression was not evenly distributed among the entire population (Fig. 1d). Flow cytometry analyses were performed to examine the expression of cellular surface markers (Fig. 2). MSCs showed remarkably uniform expression of mesenchymal markers Sca-1, CD29 and CD44. Of note, murine MSCs did not express CD90 in all four population; this is in contrast with their human counterparts, which abundantly express CD90 [15]. In addition, all four murine MSC populations uniformly expressed the perivascular marker PDGFR- $\beta$ , expression that was maintained after prolonged expansion in culture. Importantly, cells were negative for endothelial markers (CD31, CD34) and hematopoietic markers (CD45, CD11b), confirming that none of the MSC populations were contaminated with either of these additional cell types.

The ability of tissue-resident MSCs to differentiate into cells from multiple mesenchymal lineages was evaluated in vitro using well-established protocols [4]. MSCs isolated from all four murine tissues differentiated into adipocytes, osteocytes and chondrocytes, as shown by the intracellular accumulation of oil droplets (adipogenesis; Fig. 3a), expression of alkaline phosphatase and calcium deposition (osteogenesis; Fig. 3b) and glycosaminoglycan deposition in pellet cultures (chondrogenesis; Fig. 3c), respectively. Additionally, we examined the ability of each MSC population to differentiate into mature smooth muscle cells (SMCs) upon direct contact with ECs [15]. Cultured MSCs share multiple cellular markers with SMCs (e.g.,  $\alpha$ -SMA, calponin), therefore, differentiation was assessed by expression of smMHC, a definitive marker of mature SMCs that is not expressed by MSCs. Indeed, in the absence of direct contact with ECs, smMHC expression was undetectable in all MSC populations (insets in Fig. 3d). However, when MSCs were directly co-cultured with mDECs for 7 days, expression of smMHC was consistently induced in all four MSC populations (Fig. 3d), indicating smooth muscle myogenic ability. Collectively, our data showed that tissue-resident CD45<sup>-</sup>/PDGFR- $\beta$ <sup>+</sup> cells, independently isolated from the SVF of four distinct tissues, comprise a population of cells that are consistent with the definition of MSCs, as characterized via cell phenotype and multipotency.

### Pro-angiogenic potential of tissue-resident MSCs

We examined the ability of our four tissue-resident MSC populations to modulate EC behavior through secretion of paracrine pro-angiogenic factors (Fig. 4). Irrespective of the tissue origin, all four MSCs secreted multiple angiogenic factors in culture, as confirmed by examination of MSC conditioned medium (MSC-CM) using murine angiogenesis protein arrays (Fig. 4a, b). Secreted proangiogenic factors included VEGF-A, PIGF2, HGF, several members of the IGFBP family as well as matrix metallo-proteinase (MMP)-3 and -9, among other factors. Of note, murine MSCs did not secrete FGF-1 and FGF-2 (Fig. 4a), which is a distinction from human MSCs [20]. Overall, pro-angiogenic secretomes were similar in each of the MSC populations analyzed, and no particular factor was expressed exclusively in specific cell types. To examine whether MSC-secreted proteins were able to modulate EC activity, human umbilical cord blood-derived ECFCs were exposed to each MSC-CM in four different functional in vitro assays (Fig. 4c–f). First, using a standard proliferation assay, we found that all MSC-CM induced ECFC mitogenesis; cell numbers achieved after exposure to MSC-CMs for 48 h were in all cases significantly higher than those observed when cells were exposed to basal control medium (Fig. 4c). Similarly, MSC-CMs were shown to significantly increase the capacity of ECFCs to re-endothelialize scratched monolayers (Fig. 4d), to launch angiogenic sprouts (Fig. 4e), and to assemble into capillary-like structures in three-dimensional cultures (Fig. 4f). Collectively, our data indicate that tissue-resident CD45<sup>-</sup>/PDGFR- $\beta$ <sup>+</sup> MSCs from all four distinct tissues were able to modulate EC function in vitro through the secretion of paracrine factors.

## MSCs support formation of vascular networks in vivo

To examine whether tissue-resident MSCs can serve as perivascular cells and facilitate vasculogenesis in vivo, we implanted GFP-MSCs in combination with ECFCs subcutaneously into immunodeficient mice (Fig. 5a). One week after implantation, implants were removed and examined for the formation of vascular networks (Fig. 5b). H&E staining revealed that all implants had formed numerous blood vessels that were perfused and contained murine erythrocytes (Fig. 5c). Carefully examination of vessels revealed no histological evidence of either hemorrhage or thrombosis (i.e., platelet aggregation and uniform fibrin deposition), suggesting proper functionality. Quantification of average microvessel densities at day 7 revealed no statistically significant difference between implants prepared with each of the different murine MSC populations (Fig. 5d). The number of microvessels was  $124.59 \pm 13.28$  vessels/mm<sup>2</sup>,  $95.01 \pm 14.8$  vessels/mm<sup>2</sup>,  $94.99 \pm 27.53$  vessels/mm<sup>2</sup>, and  $110.94 \pm 55.65$  vessels/mm<sup>2</sup>, in implants with bmMSCs, watMSCs, skmMSCs, and myoMSCs, respectively. These values of microvessel density are similar to those previously reported with human saphenous vein SMCs, and bone marrow-derived MSCs [15, 21], indicating that all four of the murine MSCs tested were equally capable of generating extensive vascular networks.

The generation of ECFC-lined vascular structures was dependent on the presence of MSCs. Perfused vessels stained positively for human specific CD31, indicating that the newly formed human vasculature had formed functional anastomoses with murine host blood vessels (Fig. 6a). Irrespective of the MSC population used, the percentage of human vessels (hCD31<sup>+</sup>) was similar for all groups:  $60.27 \pm 8.79\%$  (bmMSCs),  $64.51 \pm 5.83\%$  (watMSCs),  $57.87 \pm 1.67\%$  (skmMSCs), and  $69.58 \pm 2.28\%$  (myo- MSCs) (Fig. 6c). The location of implanted MSCs was identified by the expression of GFP (Fig. 6a); GFP-expressing MSCs were mainly detected in proximity and immediately adjacent to luminal structures (Fig. 6a), indicating structural participation in the perivascular compartment of newly formed blood vessels. Perivascular participation of MSCs was observed in both ECFC-lined human microvessels (Fig. 6a; panels 1, 3, 5, 7) as well as in murine infiltrated host microvessels (Fig. 6a; panels 2, 4, 6, 8), and this perivascular participation took place independently of the tissue of origin from where MSCs were isolated.

Double staining of GFP and  $\alpha$ -SMA demonstrated that, after 7 days in vivo, all blood vessels inside the implants were surrounded by  $\alpha$ -SMA-positive perivascular cells (Fig. 6b). A large percentage of these perivascular  $\alpha$ -SMA-expressing cells also expressed GFP (Fig. 6b; panels 2, 4, 6, 8), confirming that donor MSCs indeed contributed to the perivascular compartment of blood vessels. Specifically, the percentage of vessels that stained positively for both  $\alpha$ -SMA and GFP was  $80.04 \pm 4.77\%$ ,  $80.14 \pm 4.32\%$ ,  $93.75 \pm 3.99\%$ , and  $75.02 \pm 9.57\%$ , in implants that used bmMSCs, watMSCs, skmMSCs, and myoMSCs, respectively (Fig. 6d). Again, no significant difference was observed between implants prepared with different MSC sources.

## Discussion

For decades, MSCs have been the subject of intensive research due to their promise in regenerative medicine [2]. Over the years, numerous studies have routinely demonstrated the capacity of MSCs to generate multiple end-stage mesenchymal cell types [2, 4]. Additionally, the presence of MSCs in the stromal vascular fraction of several adult tissues has been recently recognized [6, 7]. However, there are still aspects of MSC biology and their role in tissue homeostasis that are not fully understood [8], including the capacity to modulate the formation of blood vessels in vivo. Studies have shown the MSCs obtained from both bone marrow and subcutaneous adipose tissue facilitate the formation of blood vessels in animal models of human EC transplantation [15–17]. However, it is still unclear

whether this vascular modulatory capacity is ubiquitous to all MSCs irrespective of their tissue of origin. Here, we have demonstrated that MSCs isolated from four distinct tissues (bone marrow, adipose, skeletal muscle, and myocardium) were equally capable of supporting de novo formation of human microvascular networks. In all four tissue-resident MSCs tested, co-implantation with ECFCs into immunodeficient mice rapidly generated an extensive network of blood vessels with ECFCs specifically lining the lumens and MSCs occupying perivascular positions. Moreover, MSCs were critical for the self-assembly of ECFCs into functional capillaries, results that are in line with recent studies that showed vasculogenesis to be dependent on the presence of perivascular cells [15–17].

In the last decade, several studies have revealed that MSC identity and anatomical localization in vivo is closely related to those of perivascular cells [6, 8, 22, 23], which has prompted some investigators to propose that all MSCs are pericytes [9]. This perivascular identity has enabled the selection of MSCs to be based on pericyte markers such as PDGFR- $\beta$  and NG<sub>2</sub> [8, 24]. In the present study, we isolated MSCs from the SVF of four distinct tissues based on their expression of PDGFR- $\beta$ . Hematopoietic (CD45<sup>+</sup>) and non-perivascular (PDGFR- $\beta$ <sup>-</sup>) cells were removed using magnetic activated cell sorting (MACS). The isolated MSCs (CD45<sup>-</sup>/PDGFR- $\beta$ <sup>+</sup>) comprised a single phenotypic population (>96 % homogeneous at passages 1) by flow cytometric analysis of expressed surface antigens, including PDGFR- $\beta$ , Sca-1, CD29, and CD44. In addition, cultured MSCs uniformly lacked surface markers of hematopoietic (CD45, CD11b) and endothelial (CD31, CD34) cells, confirming they were not contaminated by these other components of the stroma. Of note, none of the four MSCs expressed CD90, which is in line with previous studies with murine MSCs [25–27]; nevertheless, positive expression of CD90 has also been reported by others [7, 28], which suggest that expression of this particular cell marker may be influenced by specific culture conditions and techniques. The phenotypes of the selected MSCs were further confirmed by evaluation of their multilineage differentiation potential. Without exception, all four MSCs populations were able to undergo adipogenesis, osteogenesis, chondrogenesis, and smooth muscle myogenesis in vitro. Collectively, all the tissue-resident MSCs described here, independently of the tissue of origin, shared the following phenotypical characteristics: (1) ability to proliferate in culture with a distinct spindle-shape morphology, (2) uniform expression of a set of surface protein markers, and (3) capacity to differentiate into multiple mesenchymal lineages under controlled in vitro conditions.

The therapeutic potential of MSCs contributes to additional trophic activities, including the ability to support the formation of vascular structures [14]. Heterotypic interactions between endothelial and mesenchymal cells in the context of blood vessel formation and stabilization have been long recognized [20, 29–31]. However, whether MSCs obtained from different tissues have different vascular modulatory properties is largely unknown. In this study, we demonstrated that several pro-angiogenic properties were ubiquitous to all tissue-resident MSCs investigated, irrespective of their original anatomical location. All MSCs secreted a plethora of pro-angiogenic factors in culture, including members of the VEGF and angiopoietin families. Collectively, these secreted pro-angiogenic factors demonstrated function in that media conditioned by MSCs unequivocally induced ECFC proliferation, migration, and sprout and tube formation in vitro.

The capacity of MSCs to modulate EC behavior was also examined in vivo. Previously, we and others demonstrated that bmMSCs facilitate the self-assembly of ECs into functional, long-lasting capillaries after implantation into immunodeficient mice [15, 16]. Other studies have shown that end-stage mesenchymal cells such as fibroblasts facilitate the assembly of ECs into blood vessels [32], although whether fibroblast can differentiate in vivo into functional pericytes that assure stable, long-lasting vasculature may need further



examination. Other authors described similar vascular modulatory properties with adipose stromal cells (ASCs), which share many of the characteristics herein used to define MSCs, including multipotent differentiation and pericytic properties [17]. However, how various MSCs differ in their capacity to facilitate vasculogenesis has not been systematically studied. To address whether this modulatory capacity is shared by all tissue-resident MSCs, we analyzed MSCs from bone marrow, white adipose tissue, and two myogenic tissues: skeletal muscle and myocardium. As expected from their similar pro-angiogenic characteristics, all four MSCs facilitated formation of vascular networks in our murine model of ECFC transplantation. Moreover, we found no statistically significant difference in either the total number of microvessels or the percentage of human ECFC-lined vessels inside the implants. Importantly, these experiments confirmed that implantation of ECFCs alone (without perivascular cells) did not generate perfused microvessels, as demonstrated in previous studies [15, 21]. In addition to the capacity to support vasculogenesis, we identified further similarities among the four MSC populations. In all cases, implanted MSCs engrafted as perivascular cells and were found tightly surrounding the majority of microvessels. There were no statistically significant differences in the percentage of vessels that were surrounded by donor MSCs expressing  $\alpha$ -SMA. MSCs were also found interstitially distributed throughout the implants in all four groups; however, whether there were any differences between the MSCs that engrafted interstitially or perivascularly remains to be elucidated. Finally, MSCs were also found to contribute to the perivascular compartment of infiltrating host microvessels, indicating that this ubiquitous MSC capacity to engraft as perivascular cells was not limited to those microvessels formed de novo.

In conclusion, we demonstrated that tissue-resident MSCs isolated from four distinct tissues have equal capacity to modulate EC function, including de novo formation of vascular networks in vivo. Our studies suggest that the capacity to modulate the formation of vasculature is an ubiquitous property of all MSCs, irrespective of their original anatomical location. Further research is warranted to determine whether this ability to support vasculogenesis is also present in other MSCs from additional postnatal tissues. Our results validate multiple tissues as potential sources of MSCs for future cell-based vascular therapies.

## Supplementary Material

Refer to Web version on PubMed Central for supplementary material.

## Acknowledgments

Mouse dermal endothelial cells (mDEC) were kindly provided by Dr. Andrew C. Dudley (University of North Carolina at Chapel Hill). Histology was supported by the Specialized Research Pathology Cores, Longwood Facility of the Dana-Farber/Harvard Cancer Center. This work was supported by a grant from the National Institutes of Health (R00EB009096) to J.M.-M, and by grants from the Instituto de Salud Carlos III and Junta de Andalucía, Consejería de Salud to R.M.-L.

## References

1. Caplan AI. Adult mesenchymal stem cells for tissue engineering versus regenerative medicine. *J Cell Physiol.* 2007; 213:341–347. [PubMed: 17620285]
2. Caplan AI, Bruder SP. Mesenchymal stem cells: building blocks for molecular medicine in the 21st century. *Trends Mol Med.* 2001; 7:259–264. [PubMed: 11378515]
3. Friedenstein AJ, Chailakhjan RK, Lalykina KS. The development of fibroblast colonies in monolayer cultures of guinea-pig bone marrow and spleen cells. *Cell Tissue Kinet.* 1970; 3:393–403. [PubMed: 5523063]

4. Pittenger MF, Mackay AM, Beck SC, et al. Multilineage potential of adult human mesenchymal stem cells. *Science*. 1999; 284:143–147. [PubMed: 10102814]
5. Prockop DJ. Marrow stromal cells as stem cells for nonhematopoietic tissues. *Science*. 1997; 276:71–74. [PubMed: 9082988]
6. Crisan M, Yap S, Casteilla L, et al. A perivascular origin for mesenchymal stem cells in multiple human organs. *Cell Stem Cell*. 2008; 3:301–313. [PubMed: 18786417]
7. Meirelles L, Chagastelles P. Mesenchymal stem cells reside in virtually all post-natal organs and tissues. *J Cell Sci*. 2006; 119(Pt 11):2204–2213. [PubMed: 16684817]
8. Nombela-Arrieta C, Ritz J, Silberstein LE. The elusive nature and function of mesenchymal stem cells. *Nat Rev Mol Cell Biol*. 2011; 12:126–131. [PubMed: 21253000]
9. Caplan AI. All MSCs are pericytes? *Cell Stem Cell*. 2008; 3:229–230. [PubMed: 18786406]
10. Estes BT, Wu AW, Guilak F. Potent induction of chondrocytic differentiation of human adipose-derived adult stem cells by bone morphogenetic protein 6. *Arthritis Rheum*. 2006; 54:1222–1232. [PubMed: 16572454]
11. Lee RH, Kim B, Choi I, et al. Characterization and expression analysis of mesenchymal stem cells from human bone marrow and adipose tissue. *Cell Physiol Biochem*. 2004; 14:311–324. [PubMed: 15319535]
12. Kaltz N, Ringe J, Holzwarth C, et al. Novel markers of mesenchymal stem cells defined by genome-wide gene expression analysis of stromal cells from different sources. *Exp Cell Res*. 2010; 316:2609–2617. [PubMed: 20599957]
13. Panepucci RA, Siufi JLC, Silva WA, et al. Comparison of gene expression of umbilical cord vein and bone marrow-derived mesenchymal stem cells. *Stem cells*. 2004; 22:1263–1278. [PubMed: 15579645]
14. Caplan AI. The Cornea D. The MSC: an injury drugstore. *Cell Stem Cell*. 2011; 9:11–15. [PubMed: 21726829]
15. Melero-Martin JM, Kang S-Y, Khan ZA, et al. Engineering robust and functional vascular networks in vivo with human adult and cord blood-derived progenitor cells. *Circ Res*. 2008; 103:194–202. [PubMed: 18556575]
16. Au P, Tam J, Fukumura D, et al. Bone marrow-derived mesenchymal stem cells facilitate engineering of long-lasting functional vasculature. *Blood*. 2008; 111:4551–4558. [PubMed: 18256324]
17. Traktuev DO, Prater DN, Merfeld-Clauss S, et al. Robust functional vascular network formation in vivo by cooperation of adipose progenitor and endothelial cells. *Circ Res*. 2009; 104:1410–1420. [PubMed: 19443841]
18. Lin R-Z, Dreyzin A, Aamodt K, et al. Functional endothelial progenitor cells from cryopreserved umbilical cord blood. *Cell Transplant*. 2011; 20:515–522. [PubMed: 20887663]
19. Lin R-Z, Dreyzin A, Aamodt K, et al. Induction of erythropoiesis using human vascular networks genetically engineered for controlled erythropoietin release. *Blood*. 2011; 118:5420–5428. [PubMed: 21937702]
20. Kinnaird T, Stabile E, Burnett MS, et al. Marrow-derived stromal cells express genes encoding a broad spectrum of arteriogenic cytokines and promote in vitro and in vivo arteriogenesis through paracrine mechanisms. *Circ Res*. 2004; 94:678–685. [PubMed: 14739163]
21. Melero-Martin JM, Khan ZA, Picard A, et al. In vivo vasculogenic potential of human blood-derived endothelial progenitor cells. *Blood*. 2007; 109:4761–4768. [PubMed: 17327403]
22. Tang W, Zeve D, Suh JM, et al. White fat progenitor cells reside in the adipose vasculature. *Science*. 2008; 322:583–586. [PubMed: 18801968]
23. Dellavalle A, Sampaolesi M, Tonlorenzi R, et al. Pericytes of human skeletal muscle are myogenic precursors distinct from satellite cells. *Nat Cell Biol*. 2007; 9:255–267. [PubMed: 17293855]
24. Schwab KE, Gargett CE. Co-expression of two perivascular cell markers isolates mesenchymal stem-like cells from human endometrium. *Hum Reprod*. 2007; 22:2903–2911. [PubMed: 17872908]
25. Anjos-Afonso F, Siapati EK, Bonnet D. In vivo contribution of murine mesenchymal stem cells into multiple cell-types under minimal damage conditions. *J Cell Sci*. 2004; 117:5655–5664. [PubMed: 15494370]

26. Peister A, Mellad JA, Larson BL, et al. Adult stem cells from bone marrow (MSCs) isolated from different strains of inbred mice vary in surface epitopes, rates of proliferation, and differentiation potential. *Blood*. 2004; 103:1662–1668. [PubMed: 14592819]
27. Suire C, Brouard N, Hirschi K, et al. Isolation of the stromal-vascular fraction of mouse bone marrow markedly enhances the yield of clonogenic stromal progenitors. *Blood*. 2012; 119:e86–e95. [PubMed: 22262767]
28. Bi Y, Ehrichtou D, Kilts TM, et al. Identification of tendon stem/progenitor cells and the role of the extracellular matrix in their niche. *Nat Med*. 2007; 13:1219–1227. [PubMed: 17828274]
29. Antonelli-Orlidge A, Saunders KB, Smith SR, et al. An activated form of transforming growth factor beta is produced by cocultures of endothelial cells and pericytes. *Proc Natl Acad Sci USA*. 1989; 86:4544–4548. [PubMed: 2734305]
30. Folkman J, D'Amore PA. Blood vessel formation: what is its molecular basis? *Cell*. 1996; 87:1153–1155. [PubMed: 8980221]
31. Jain RK. Molecular regulation of vessel maturation. *Nat Med*. 2003; 9:685–693. [PubMed: 12778167]
32. Chen X, Aledia AS, Popson SA, et al. Rapid anastomosis of endothelial precursor cell-derived vessels with host vasculature is promoted by a high density of co-transplanted fibroblasts. *Tissue Eng Part A*. 2010; 16:585–594. [PubMed: 19737050]

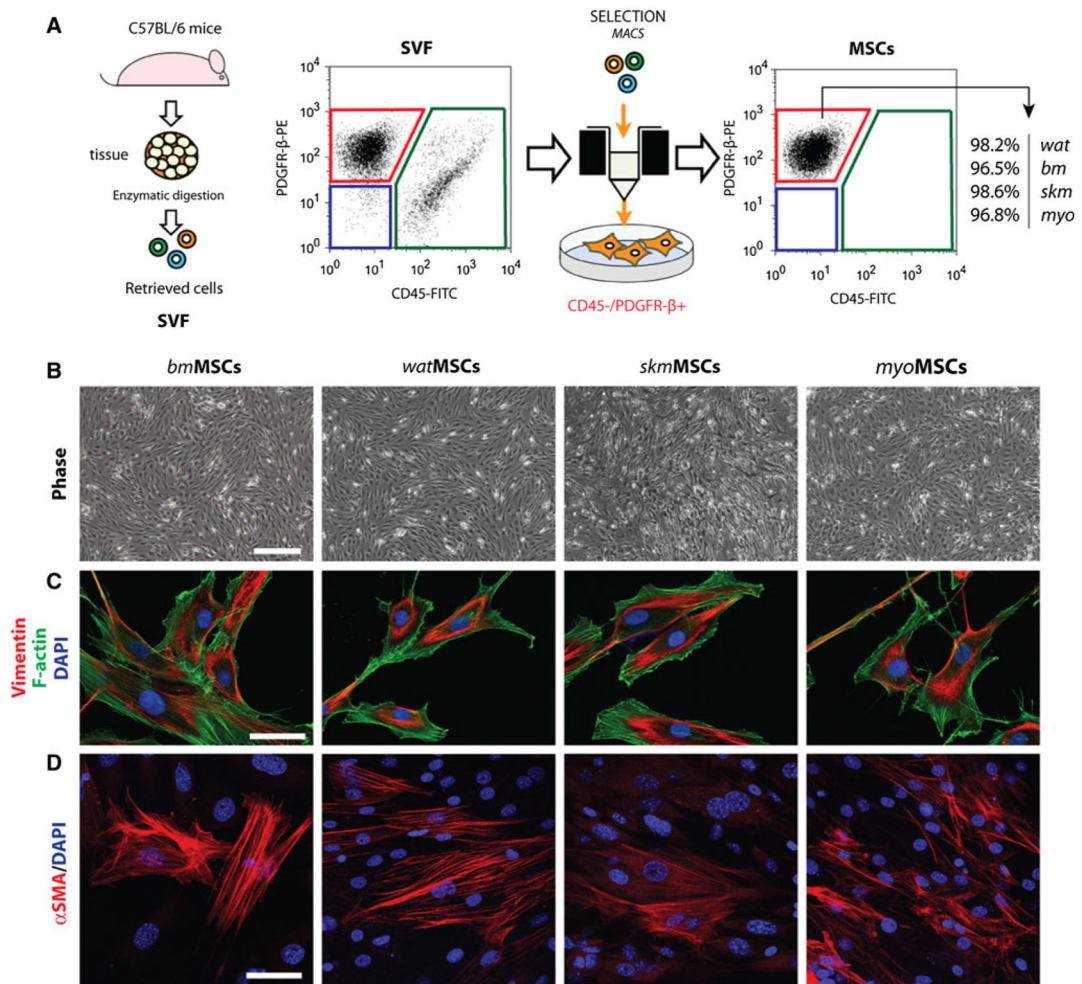


**Fig. 1.** Isolation and characterization of MSCs from four different murine tissues. **a** Tissue-resident MSCs were isolated from the stromal vascular fraction (SVF) of four different murine tissues: white adipose tissue (wat), bone marrow (bm), skeletal muscle (skm), myocardium (myo). MSCs were selected based on their negative expression of CD45 and positive expression of PDGFR- $\beta$  using magnetic activated cell sorting (MACS). **b** Phase-contrast micrographs of confluent MSCs after 3 passages in culture (*scale bar* 100  $\mu$ m). **c** Indirect immunofluorescent staining of MSCs using an anti-vimentin antibody. Cells were counterstained with phalloidin for F-actin filaments and DAPI for nuclei (*scale bar* 20  $\mu$ m) **d** Immunofluorescent staining of MSCs using an anti- $\alpha$ -SMA antibody and DAPI (*scale bar* 20  $\mu$ m)

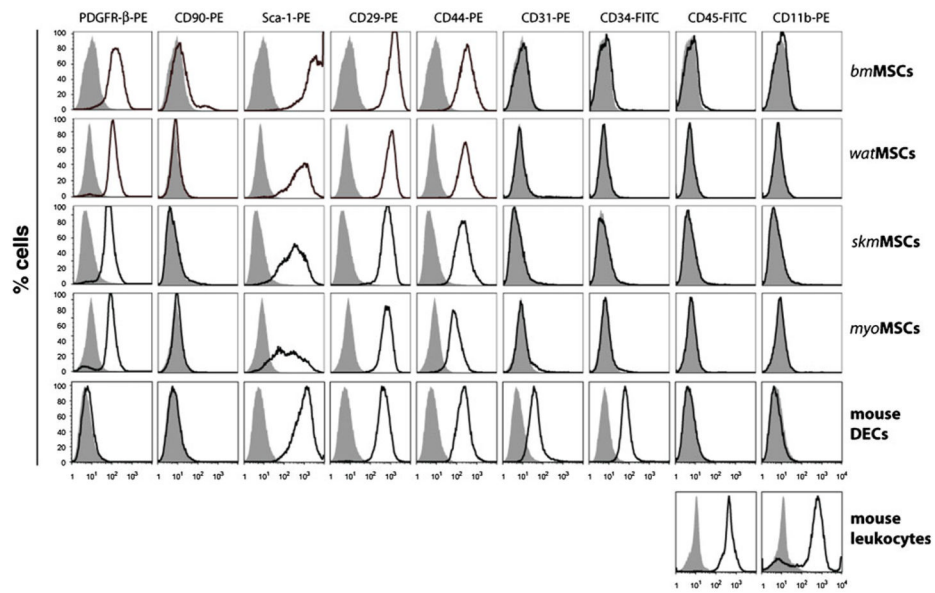


**Fig. 2.** Cytometric analysis of cultured MSCs. Expression of surface markers PDGFR- $\beta$ , CD90, Sca-1, CD29, CD44, CD31, CD34, CD45 and CD11b was analyzed by flow cytometry. *Black-lined histograms* represent cells stained with fluorescent antibodies. Isotype-matched controls are overlaid in solid grey histograms. Murine dermal endothelial cells (mDECs) and peripheral blood leukocytes served as endothelial and hematopoietic controls, respectively

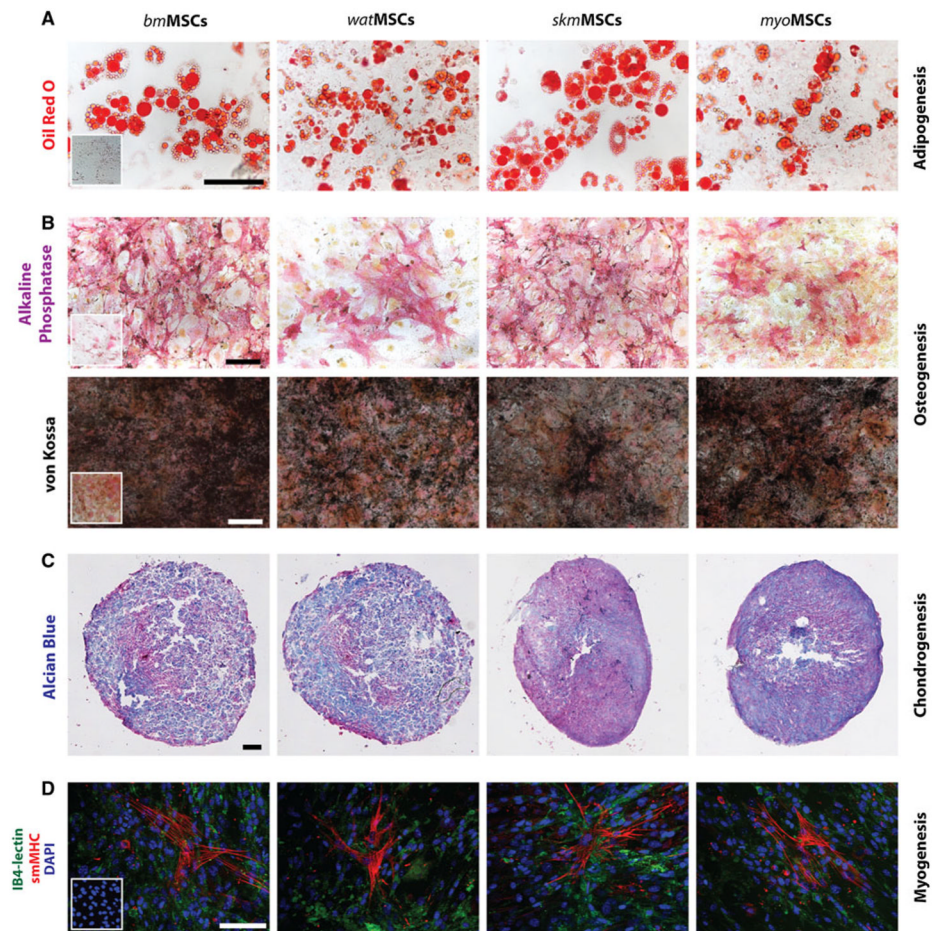


**Fig. 3.** Multilineage differentiation of MSCs. **a** Differentiation into adipocytes was revealed by oil red O staining (*scale bar* 100  $\mu\text{m}$ ). **b** Differentiation into osteocytes was revealed by alkaline phosphatase staining as well as von Kossa staining for calcium mineralization (*scale bar* 100  $\mu\text{m}$ ). *Insets* represent MSCs in non-differentiating control medium. **c** Chondrogenic differentiation was revealed in pellet culture by the presence of glycosaminoglycans, detected by Alcian blue staining (*scale bar* 200  $\mu\text{m}$ ). **d** Smooth muscle cell (SMC) differentiation was evaluated by culturing MSCs in the presence of murine mDECs for 7 days. Induction of SMC phenotype was assessed by the expression of smooth muscle myosin heavy chain (smMHC). IB4-FITC lectin was used to stain mDECs and DAPI for cell nuclei (*scale bar* 100  $\mu\text{m}$ ). *Inset* represents MSCs cultured in the absence of mDECs

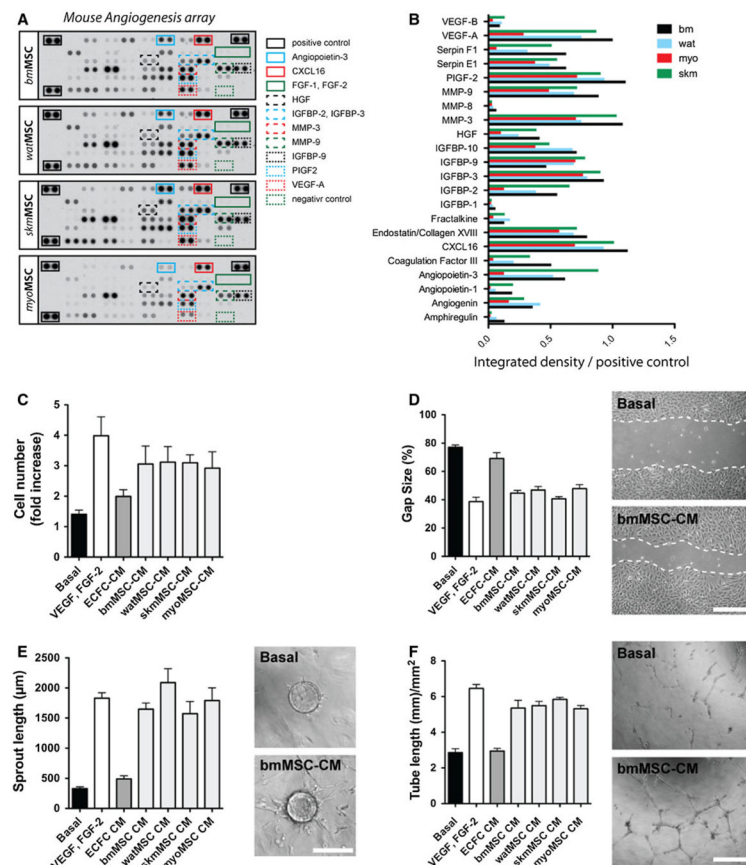


**Fig. 4.**

Pro-angiogenic properties of MSCs. **a** Murine angiogenesis protein array analysis of medium conditioned by MSCs (MSC-CM) for 24 h. The position of selected angiogenic factors in the membranes is marked with *color-lined boxes*. **b** Quantification of selected angiogenic factors in MSC-CM was carried out by densitometry. **c** Proliferation of ECFCs after 48 h in the presence of MSCCM. **d** Scratch size (% original size) on a confluent layer of ECFCs after 48 h in the presence of MSC-CM (*scale bar* 500  $\mu\text{m}$ ). **e** Total sprout length from ECFC-coated Cytodex-3 microcarriers embedded in fibrin gel for 4 days in the presence of MSC-CM (*scale bar*: 200  $\mu\text{m}$ ). **f** Total tube length formed by ECFCs cultured on Matrigel-coated plates for 24 h in the presence of MSC-CM (*scale bar* 500  $\mu\text{m}$ ). Basal medium, VEGF-A(10 ng/mL)/bFGF(1 ng/mL), and ECFC-CM served as control (C-F). *Bars* represent mean values determined from three replicate samples  $\pm$  SEM

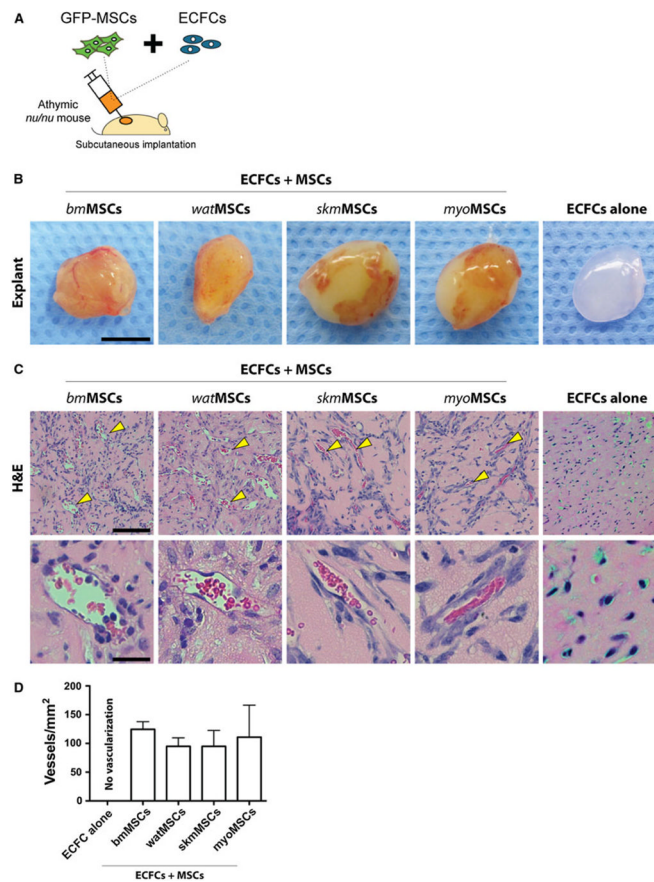


**Fig. 5.** Pro-vasculogenic properties of MSCs. **a** MSCs isolated from four different GFP-C57BL/6 murine tissues (GFP-MSCs) were combined with ECFCs ( $2 \times 10^6$  total; 40:60 ECFC/GFP-MSC ratio) in 200  $\mu$ L of Matrigel and the mixture was subcutaneously injected into nu/nu mice ( $n = 4$  for each MSC group). Implants containing ECFCs alone served as controls. **b** Macroscopic views of representative Matrigel explants at day 7 (*scale bar* 5 mm). **c** H&E staining at day 7 revealed the presence of numerous blood vessels containing erythrocytes (*yellow arrowheads*). Top panels (*scale bars* 100  $\mu$ m) and bottom panels (*scale bars* 20  $\mu$ m) are images at low and high magnification, respectively. **d** Microvessel density was determined at day 7 by counting luminal structures containing erythrocytes. *Bars* represent the mean microvessel density determined from four replicate implants  $\pm$  SEM



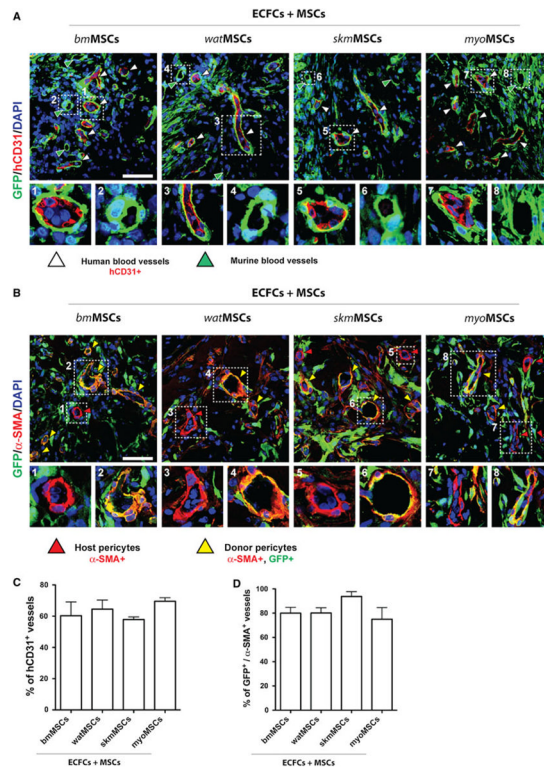


**Fig. 6.** Perivascular engraftment of MSCs. GFP-MSCs obtained from four different murine tissues were combined with ECFCs ( $2 \times 10^6$  total; 40:60 ECFC/GFP-MSC ratio) in 200  $\mu$ L of Matrigel and the mixture subcutaneously injected into nu/nu mice ( $n = 4$  for each MSC group). **a** Immunofluorescent staining of engrafted MSCs and ECFCs using anti-GFP and anti-human CD31 antibodies, respectively. White arrowheads indicate hCD31<sup>+</sup>, ECFC-lined vessels. High magnification of selected regions showing representative human (panels 1, 3, 5, 7) and mouse (panels 2, 4, 6, 8) blood vessels that were covered by perivascular GFP-MSCs. **b** Immunofluorescent staining of engrafted MSCs and perivascular cells using anti-GFP and anti- $\alpha$ -SMA antibodies, respectively.  $\alpha$ -SMA-expressing perivascular cells were either donor GFP<sup>+</sup> MSCs (yellow arrowheads) or GFP<sup>-</sup> host cells (red arrowheads). High magnification of selected regions showing representative blood vessels with GFP<sup>+</sup> donor (panels 2, 4, 6, 8) and GFP<sup>-</sup> host (panels 1, 3, 5, 7) perivascular cells. All images are representative of explants from four different mice. Nuclei were counterstained with DAPI. (scale bars 50  $\mu$ m). **c** Percentage of blood vessels that were lined by hCD31<sup>+</sup> ECFCs. **d** Percentage of blood vessels with perivascular cells that expressed both GFP and  $\alpha$ -SMA. Bars represent mean values determined from four replicate implants  $\pm$  SEM